



A novel bonding of 6,7-dichloroquinoxaline-2,3-dione, DCQX, to two molybdenum (0) metal centers: Synthesis, characterization, biological activity studies and semiempirical calculations of $[(bpy)_2Mo(\mu_2-\kappa^2:\eta^6-DCQX)Mo(CO)_3]$ complex

Attia S. Attia*, Ayman A. Abdel Aziz, Khalifa A. Alfallous, M.F. El-Shahat

Chemistry Department, Faculty of Science, Ain Shams University, Abbasia, Cairo 11566, Egypt

ARTICLE INFO

Article history:

Received 29 May 2012

Accepted 8 July 2012

Available online 17 July 2012

Keywords:

Quinoxaline

Molybdenum complex

Metal carbonyl

Bipyridine

Semiempirical calculations

Biological activity

ABSTRACT

A complex of the general formula $Mo_2(bpy)_2(DCQX)(CO)_3$, (where DCQX and bpy are 6,7-dichloroquinoxaline-2,3-dione and 2,2'-bipyridine), was synthesized in two steps starting with the reaction of $Mo(CO)_6$ with bpy then followed by the addition of DCQX ligand. Initial characterization based on the elemental and mass analyses has suggested three possible structures (**1–3**). In the three suggested structures the DCQX ligand bonded to two Mo(0) metal centers; to one Mo metal through its C=O functional groups and the other through the aromatic ring forming η^6 -arene type. In structure **1** the DCQX ligands bonded to $(bpy)_2Mo$ and $Mo(CO)_3$ moieties, whereas in the other structures the DCQX ligands bonded to Mo $(bpy)(CO)$ and *cis*- $(bpy)(CO)_2Mo$ (**2**) or *trans*- $(bpy)(CO)_2Mo$ (**3**) moieties. The IR studies were useful in assigning the coordination modes of the ligands especially in the carbonyl region of the spectrum. 1H NMR studies in $DMSO-d_6$ displayed typical patterns corresponding to *cis*- $(bpy)_2M$ moiety. The electronic absorption spectrum of the complex revealed two bands assignable to $Mo(d_{\pi}) \rightarrow arene(\pi^*)$ and $Mo(d_{\pi}) \rightarrow bpy(\pi^*)$ MLCT transitions. The thermogravimetric analysis gave more insight into the composition and the thermal stability of the complex. The structural and vibrational behaviors of the $Mo_2(bpy)_2(DCQX)(CO)_3$ complex have been elucidated using semiempirical parameterized PM3 method. Although, both DCQX ligand and the molybdenum complex showed antimicrobial activities, the complex inhibition to the studied microorganisms was higher.

© 2012 Elsevier Ltd. All rights reserved.

1. Introduction

Quinoxalines represent an important class of heterocyclic compounds. Several quinoxaline derivatives are associated with a wide range of biological activities behaving as anticancer, antiviral, and antibacterial, in addition to activity as kinase inhibitors [1–4]. Also quinoxaline ring is part of a number of synthetic antibiotics such as echinomycin, leromycin, and actinomycin, which are known to inhibit the growth of gram-positive bacteria and are also active against various transplantable tumors [5–7].

More than half a century ago, Dwyer and coworkers [8–12] started to investigate the biological activities of simple coordination complexes such as ruthenium complexes with 2,2'-bipyridine (bpy) and 1,10-phenanthroline (phen) ligands. He discovered that some very hydrophobic complexes displayed bacteriostatic and bactericidal activities and were capable of inhibiting tumor growth

[9,10]. Recently, Meggers and coworkers [13–15] have developed organoruthenium compounds as protein kinase inhibitors. Their work demonstrated how organometallic compounds of the type $(arene)M(N-N)CO$ can make use of their unique structural opportunities to fill an enzyme active site and inhibit tumor growth.

This rich area of research work has prompted us to design a complex containing quinoxaline, $(bpy)M$ and $(\eta^6-arene)M$ moieties. In the present work, we describe the synthesis of a novel complex containing 6,7-dichloroquinoxaline-2,3-dione ligand that coordinates to $(bpy)_2Mo$ and $Mo(CO)_3$ moieties through its C=O and aromatic ring, respectively. Spectral, thermal and electronic studies are described as well to give more insight into the synthesized complex. In addition, semiempirical theoretical calculations (MM+ and parameterized PM3) were used to predict the most stable structure of the $Mo_2(bpy)_2(DCQX)(CO)_3$ complex and to calculate its vibrational frequencies. Finally, the antimicrobial activities of the DCQX ligand and the $Mo_2(bpy)_2(DCQX)(CO)_3$ complex were studied to provide information about their inhibition activities against bacteria and fungi.

* Corresponding author. Tel.: +20 2 6717 839.

E-mail address: attiasattia@hotmail.com (A.S. Attia).

2. Experimental

Molybdenum hexacarbonyl ($\text{Mo}(\text{CO})_6$), 2,2'-bipyridine (bpy), oxalic acid ($\text{C}_2\text{H}_2\text{O}_4 \cdot 2\text{H}_2\text{O}$) and 4,5-dichloro-1,2-phenylenediamine ($\text{C}_6\text{H}_6\text{N}_2\text{Cl}_2$) were used as purchased from Sigma–Aldrich Chemical Co. Inc. 6,7-dichloroquinoxaline-2,3-dione (DCQX) ligand was synthesized following the reported procedure [16]. All Solvents used were dried according to standard procedures.

Elemental analyses were performed using a Perkin–Elmer 2400 CHN elemental analyzer. Mass Spectra were obtained on a JEOL JMS-AX500 mass spectrometer. Thermogravimetric analysis (TGA) was carried out on a solid sample, under nitrogen atmosphere with a heating rate of $10^\circ\text{C}/\text{min}$., using Shimadzu DT-50 thermal analyzer. ^1H NMR spectra were performed on a JEOL-270 MHz NMR spectrometer in $\text{DMSO}-d_6$ solvent and TMS was used as an internal reference. Infrared spectra ($4000\text{--}400\text{ cm}^{-1}$) were recorded as KBr pellets on a Unicam Masttson 1000 FTIR spectrometer. The electronic absorption spectra were recorded by using Unicam UV2–300 UV–Vis spectrometer. Samples of $2\text{--}6 \times 10^{-4}\text{ mol dm}^{-3}$ concentrations in DMSO were measured against the solvent in the reference cell.

Antimicrobial activity of the tested samples for the ligand and the complex was determined using a modified Kirby–Bauer disc diffusion method [17]. A $100\ \mu\text{L}$ of the test bacteria or fungi were grown in 10 mL of fresh media until they reach a count of an approximately 108 cells/mL for bacteria and an approximately 105 cells/mL for fungi. A $100\ 100\ \mu\text{L}$ of microbial suspension was spread onto agar plates corresponding to the broth in which they were maintained. Plates inoculated with Gram-positive bacteria (*Staphylococcus aureus*) and Gram-negative bacteria (*Escherichia Coli*) were incubated at $35\text{--}37^\circ\text{C}$ for 24–48 h. Whereas, filamentous fungus (*Aspergillus flavus*) and yeast fungus (*Candida albicans*) were incubated at 25°C for 48 h and 30°C for 24–48 h, respectively. Then the diameters of the inhibition zones were measured in millimeters. Standard discs of tetracycline (antibacterial agent) and Amphotericin (antifungal agent) served as positive control for antimicrobial activity, while filter discs impregnated with $10\ \mu\text{L}$ of DMSO solvent were used as a negative control. Blank paper discs with a diameter of 8.0 mm were impregnated with $10\ \mu\text{L}$ of the tested samples stock solution (0.02 g/mL) and inhibition zone diameters were measured.

The semiempirical calculations in this study have been carried out using the Hyperchem 6.01 program package [18]. The Polak–Ribiere version of the conjugate gradient method was used in all energy minimization calculations with a coverage criterion less than $0.0001\text{ kcal mol}^{-1}\ \text{\AA}^{-1}$. First and separately DCQX and bpy ligand have been optimized and the results obtained have been applied in each calculation thereafter. The values of Mo–O, Mo–N, Mo–C (arene) and Mo–C (carbonyl) bond lengths and angles in the literatures were used as the starting inputs [19–23]. Initial optimization of the complexes was performed with molecular mechanics (MM+). The geometry was further refined using parameterized PM3 method. Available parameters for Mo metal were implemented in PM3 semiempirical method [24]. The parameterized PM3 was used for geometry optimization of the complexes under study. Singlet state RHF spin pairing has been selected in addition the standard SCF (with accelerated convergence). Theoretical harmonic vibrational frequencies are related to the experimental fundamentals by optimum scaling factor λ determined through a least-squares procedure giving by $\lambda = \sum_i^{all} \omega_i^{theor} v_i^{exp t} / \sum_i^{all} (\omega_i^{theor})^2$, where ω_i^{theor} and $v_i^{exp t}$ are the *i*th theoretical harmonic and *i*th experimental fundamental frequencies (in cm^{-1}) [25]. The molecular root mean square error (rms) was calculated by the square root of the sum over all the modes of Δ_{min} given in reference 25, where Δ_{min} is the minimized residual for each mode.

2.1. Synthesis of $\text{Mo}_2(\text{bpy})_2(\text{DCQX})(\text{CO})_3$ complex

A solution 2,2'-bipyridine (0.088 g, 0.563 mmol) in dry THF was added to a solution of molybdenum hexacarbonyl (0.150 g, 0.568 mmol) under nitrogen in Schlenk flask. The resulting solution was stirred at the reflux temperature for 30 min. The light red colored solution obtained was cooled down to room temperature, and then a THF solution of DCQX (0.072 g, 0.312 mmol) was transferred to the reaction medium under nitrogen atmosphere. The reaction mixture was heated again to reflux temperature for 15 h and kept away from light. During this time, a dark brown solid of the product has separated from the solution and was isolated by filtration, then washed several times with THF and dried under vacuum. A slow diffusion of concentrated DMF solution of the crude solid into THF solvent has resulted in light brown microcrystals of the complex. The crystals were dried under vacuum overnight and gave 0.132 g of the product (57.3% yield).

Anal. Calc. for $\text{C}_{31}\text{H}_{20}\text{Cl}_2\text{Mo}_2\text{N}_6\text{O}_5$ ($M_r = 819.31$): C, 45.44; H, 2.46; Cl, 8.65; N, 10.26. Found: C, 45.41; H, 2.47; Cl, 8.63; N, 10.30%.

3. Results and discussion

Thermal reaction of $\text{Mo}(\text{CO})_6$ with 2,2'-bipyridine followed by addition of DCQX ligand has resulted in a dinuclear molybdenum complex. Initial characterization of the complex based on the elemental analysis data has indicated the presence of a complex with the general formula; $\text{Mo}_2(\text{bpy})_2(\text{DCQX})(\text{CO})_3$.

The mass spectrum of the dinuclear molybdenum complex shown in Fig. 1, exhibited parent peak due to molecular ions $[\text{M}]^+$ and $[\text{M}+2]^+$ at 819.4 and 821.6, respectively. Fragments corresponding to successive fragmentation of the three CO ligands were found at 791.4, 764.1 and 736.4. Peaks corresponding to successive fragmentations of the two bipyridine ligands were observed at 662.0 and 506.1. Other peaks corresponding to fragmentations of $\text{Mo}(\text{CO})_3$, $\text{Mo}(\text{bpy})$, $\text{Mo}(\text{bpy})(\text{CO})_2$ and $\text{Mo}(\text{bpy})(\text{CO})$ moieties were found at 636.7, 410.7, 510.6 and 539.0, respectively.

The analytical data and mass analysis suggest three possible structures (1–3) for the synthesized complex shown in Scheme 1. In the first step of the reaction $(\text{bpy})\text{Mo}(\text{CO})_4$ is formed [26]. Recently, Green and co-workers have shown that group 6 metal carbonyls react with diamines and diphosphines to give

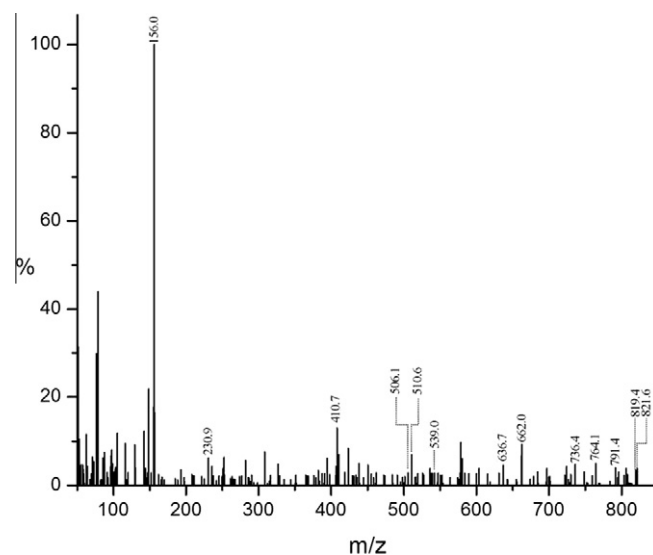
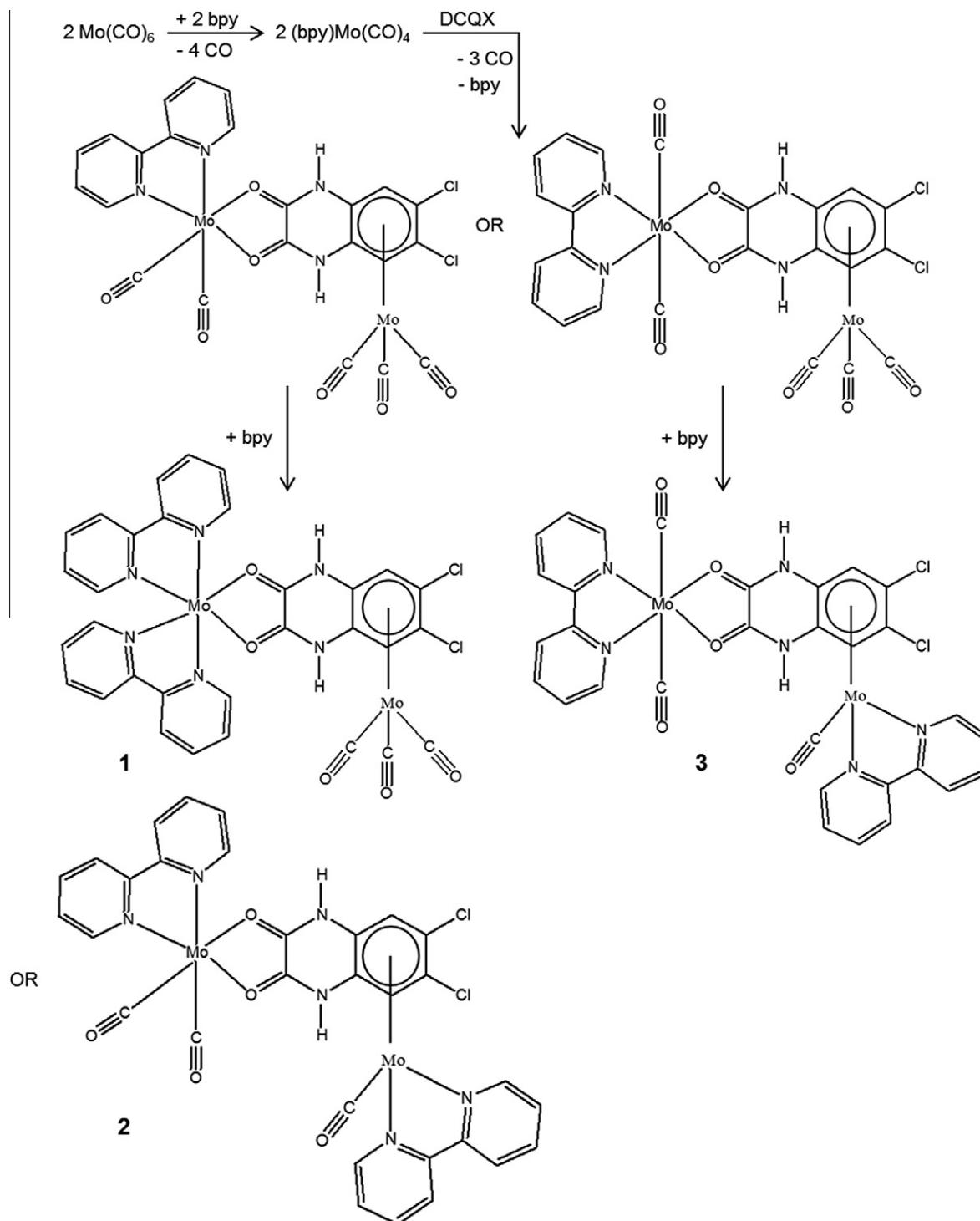


Fig. 1. The mass spectrum for $\text{Mo}_2(\text{bpy})_2(\text{DCQX})(\text{CO})_3$ complex.



Scheme 1. Suggested structures for the $\text{Mo}_2(\text{bpy})_2(\text{DCQX})(\text{CO})_3$ complex.

tetracarbonyl products, $\text{Mo(CO)}_4\text{L}$ ($\text{L} = \text{en}, \text{bpy}, \text{dppm}, \text{dppe}$), with significant enhancements of the thermal reactions [27]. Then addition of excess amount of DCQX resulted in the substitution of a bipyridine and a CO ligand of one $(\text{bpy})\text{Mo(CO)}_4$ molecule and the Mo metal binds to the aromatic ring of the DCQX ligand forming Mo-arene bond. On the other hand, DCQX can act as a bidentate ligand and coordinates through its two C=O groups to the Mo metal of another $(\text{bpy})\text{Mo(CO)}_4$ molecule by substituting two CO ligands. Two possible intermediates may result where the two CO groups arranged in a *cis* or a *trans* positions around

the Mo center. Thereafter, as the reaction proceed; the separated bpy from the second step (Scheme 1) may replace two CO of either Mo centers resulting in complexes **1–3**. Dilsky et al. [28], have reported the substitution reactions of $[(\text{bpy})(\text{MeIm})\text{M}(\text{CO})_2(\text{NO})]\text{PF}_6$ complexes ($\text{M} = \text{Mo}$ and W) that showed the bpy and MeIm ligands to be more labile than the carbonyl ligands. Whereas, attempt to displace one of the CO ligands using excess PMe_3 has resulted in substitution of both CO ligands. However, further substitution of carbonyls ligands in $\text{Mo}(\text{bpy})(\text{CO})_4$ and $\text{Mo}(\text{phen})(\text{CO})_4$ was reported to be possible and resulted in formation of *cis*- $\text{Mo}(\text{bpy})_2$

(CO)₂ and *cis*-Mo(phen)₂(CO)₂, respectively [29,30]. It is worthy to note that when the synthetic procedure was carried out in presence of light has resulted in complex decomposition after short time. This might be attributed to the decomplexing nature of the arene ring in presence of light [31]. Since only one product has obtained experimentally, therefore careful spectroscopic characterizations have to be done to assign the correct structure of the synthesized complex.

Infrared spectroscopic studies of $\nu(\text{CO})$ alone often provide valuable information about the structure and bonding of carbonyl complexes, since $\nu(\text{CO})$ is generally free from coupling with other modes and is not obscured by the presence of other vibrations [32]. The IR bands of Mo(CO)₆ were reported to appear at 2004 cm⁻¹ (CO stretch) and 660 cm⁻¹ (Mo–C stretching vibration) [32]. In addition, partial substitution of CO ligands in the Mo(CO)₆ should increase the extent of the metal d_π back-donation to the remaining CO groups; consequently the Mo–CO bond order is expected to increase and the C–O bond order of residual carbonyl ligands is expected to decrease [33]. The IR of the molybdenum complex revealed two absorption bands in carbonyl region of the spectrum at 1939.7 and 1854.0 cm⁻¹. They are consistent with the A₁ and E patterns observed for arene transition metal carbonyls [34–38]. These results are in good agreement with the suggested structure **1** and may rule out structures **2** and **3** which are expected to show absorptions corresponding the carbonyl stretching frequency of the *cis* and *trans*-(bpy)Mo(CO)₂ moiety in the 1800–1700 cm⁻¹ region, due to the strong Mo(d_π) → (π*)CO back-bonding in these dicarbonyl complexes [39,40]. Also, the IR spectroscopy was useful in assigning the coordination modes of the DCQX ligand to Mo metal centers. The IR of the free DCQX ligand revealed vibrational bands at 3416 (νN–H), 3060 and 3042 (νC–H) and 1728 (νC=O) cm⁻¹. For the complex the C=O band has shifted to lower frequency (Δν = 46 cm⁻¹), and may suggest the coordination of the DCQX ligand to the Mo metal through the unreduced C=O groups. In contrast, the stretching vibrations corresponding to the aromatic C–H group have shifted to higher frequencies at 3109 and 3079 cm⁻¹. Such behavior is consistent with that observed for C–H stretching vibration of (η⁶-benzene)Cr(CO)₃ complex compared with the free benzene itself [34]. Coordination of the bipyridine ligand to transition metals can be assigned through the shift of the stretching vibration of C=N group and the split of the 755 cm⁻¹ band, corresponding to the out-of-plane deformation mode of two equivalent sets of 4H atoms on the free bipyridine ring, by ~30 cm⁻¹ [41,42]. The IR of Mo₂(bpy)₂(DCQX)(CO)₃ displayed the band due to νC=N group of the coordinated bipyridine ligand at 1604 cm⁻¹, while those corresponding to γC–H were observed at 773 and 743 cm⁻¹.

The analytical data, mass analysis and IR spectroscopy are in good agreement with suggested structure **1**, unfortunately, there is no structural information for the synthesized complex due to the poor quality of the crystals obtained. Therefore, it is considered worthwhile to model the three suggested structures using semi-empirical parameterized PM3 method and calculate the vibrational frequencies of the most favored structure to compare them with the measured results.

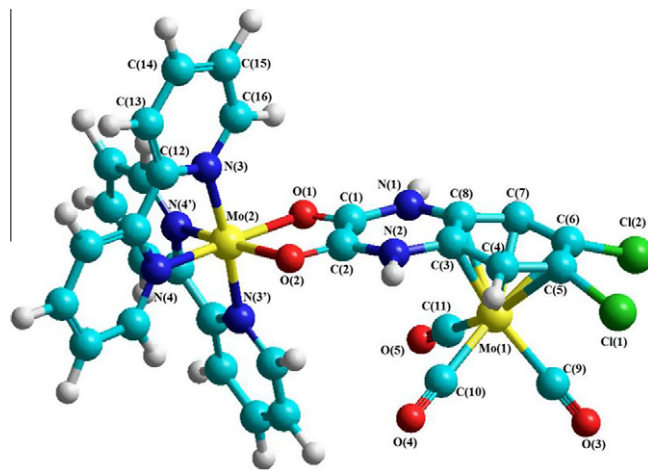
The total energy and heat of formation calculated for the suggested complexes using parameterized PM3 are summarized in Table 1. It can be seen that structure **1** is the most stable among the three suggested structures. The optimized geometry for the most favored structure of dimeric molybdenum complex is shown in Fig. 2 and the calculated bond lengths and angles are summarized in Table 2. The Mo(1) atom in Mo₂(bpy)₂(DCQX)(CO)₃ complex is bonded to the aromatic ring of DCQX and three CO ligands in arene piano-stool fashion bonding, with average bond length values for Mo–C (arene), M–C (carbonyl) and C–O of 2.210, 1.947 and 1.151 Å, respectively. The calculated values for Mo–CO and C–O

Table 1

Calculated results for the suggested structures of the Mo₂(bpy)₂(DCQX)(CO)₃ complex.

Calculation results ^a (kcal/mol)	Structure 1	Structure 2	Structure 3
Total energy	–175394.9	–175391.1	–175387.6
Heat of formation	–834.69	–830.89	–827.39

^a Total charge = 0, Spin multiplicity = 1 for all structures.

**Fig. 2.** The most stable geometry of Mo₂(bpy)₂(DCQX)(CO)₃ complex.**Table 2**

Selected bond lengths (Å) and angles (°) for Mo₂(bpy)₂(DCQX)(CO)₃ complex obtained from parameterized PM3 geometry optimization.

Bond lengths			
Carbonyls			
Mo(1)–C(9)	1.9492	C(9)–O(3)	1.1501
Mo(1)–C(10)	1.9455	C(10)–O(4)	1.1522
Mo(1)–C(11)	1.9458	C(11)–O(5)	1.1521
DCQX			
Mo(1)–C(3)	2.2355	C(3)–C(4)	1.4559
Mo(1)–C(4)	2.1829	C(4)–C(5)	1.4173
Mo(1)–C(5)	2.2004	C(5)–C(6)	1.4491
Mo(1)–C(6)	2.1972	C(6)–C(7)	1.4172
Mo(1)–C(7)	2.1847	C(7)–C(8)	1.4564
Mo(1)–C(8)	2.2409	C(8)–C(3)	1.4227
Mo(2)–O(1)	2.0171	C(1)–O(1)	1.2652
Mo(2)–O(2)	2.0174	C(2)–O(2)	1.2461
Bipyridine			
Mo(2)–N(3)	1.9933	Mo(2)–N(3')	1.9954
Mo(2)–N(4)	1.9901	Mo(2)–N(4')	1.9906
Bond angles			
C(9)–Mo(1)–C(10)	87.50	N(3')–Mo(2)–N(4')	74.81
C(10)–Mo(1)–C(11)	87.75	O(1)–Mo(2)–N(4')	169.21
C(11)–Mo(1)–C(9)	87.49	O(2)–Mo(2)–N(4)	171.65
O(1)–Mo(2)–O(2)	78.24	N(3)–Mo(2)–N(3')	174.66
N(3)–Mo(2)–N(4)	74.83		

compares well with those reported for the (η⁶-C₆H₅F)Mo(CO)₃ and (η⁶-C₆H₅CF₃)Mo(CO)₃ complexes [43]. Whereas, the average value of calculated bond length for Mo–C (arene) is shorter by 0.14–0.16 Å than those reported for (η⁶-arene)Mo(CO)₃ [19,43,44]. The calculated OC–Mo–CO bond angle in the average of 87.6° is in good agreements with those reported for structurally characterized (η⁶-arene)Mo(CO)₃ complexes; (η⁶-C₆H₅F)Mo(CO)₃ (87.5°), (η⁶-C₆H₅CF₃)Mo(CO)₃ (86.9°) and (η⁶-C₆H₅–C₆H₅)Mo(CO)₃ (85.9) [43]. A characteristic feature of arene complexes is the localization of the arene π-bonds upon coordination to metal centers [45]. This Feature can be seen, in the average short and long C–C

Table 3
Characteristic calculated and observed vibrational frequencies (cm^{-1}) for $\text{Mo}_2(\text{bpy})_2(\text{DCQX})(\text{CO})_3$ complex.

Vibrational Frequencies (cm^{-1}) ^a		Assignment
Observed	Calculated	
3431.8 (s,b)	3423.2	ν_{asymm} N–H
3109.5 (sh)	3100.9	$\nu\text{C–H}$ (arene)
3079.2 (w)	3069.9	$\nu\text{C–H}$ (arene)
1939.7 (s)	1954.6	ν_{symm} CO (carbonyl)
1845.0 (vs)	1853.0	ν_{asymm} CO (carbonyl)
1678.9 (s)	1681.7	$\nu\text{C}=\text{O}$ (DCQX)
1604.7 (m)	1610.3	$\nu\text{C}=\text{N}$ (bpy)
1545.5 (sh)	1540.8	νCC (arene ring deformation)
1470.3 (m)	1474.5	νCC (arene ring deformation)
1444.3 (s)	1446.4	νCC (arene ring deformation)
1248.8 (w)	1247.2	νCC (bpy)
1163.1 (m)	1177.3	δCC (bpy)
1112.1 (w)	1116.9	νCC (bpy)
1102.3 (w)	1102.2	δCC (bpy)
1032.3 (s)	1028.7	νCC (bpy)
961.6 (vs)	971.9	$\delta\text{C–H}$ in-plane (arene)
894.8 (w)	892.5	νCC (bpy)
843.3 (m)	846.3	$\gamma\text{C–H}$ out-of-plane (arene)
772.6 (s)	778.4	$\gamma\text{C–H}$ out-of-plane (bpy)
742. (s)	745.3	$\gamma\text{C–H}$ out-of-plane (bpy)
668.8 (m)	670.7	$\nu\text{M–C}$ (carbonyl)
421.1 (w)	425.9	$\nu\text{M–C}$ (arene)

^a w, weak; m, medium; s, strong; vs, very strong; b, broad.

bond lengths in arene ring of 1.419 and 1.454 Å, calculated for the $\text{Mo}_2(\text{bpy})(\text{DCQX})(\text{CO})_3$ complex. The values reported for $(\eta^6\text{-C}_6\text{H}_3\text{Me}_3)\text{Mo}(\text{CO})_3$ were 1.405 and 1.441 Å [44]. In the other part of the complex, Mo(2) atom is six-coordinated with two oxygen atoms from the DCQX ligand and four nitrogen atoms from two bipyridine ligands. The average Mo–O bond length calculated for the $\text{Mo}_2(\text{bpy})(\text{DCQX})(\text{CO})_3$ complex was 2.017 Å and that reported for $\text{Mo}(\text{phenCat})_2(\text{phenSQ})$ complex, containing partial and fully reduced coordinated C–O, was 1.975 Å [46]. This might support the suggested structure in which DCQX ligand is coordinated to the molybdenum metal center through unreduced form of the C=O groups. Further support is gained from the calculated C=O bond length in the average of 1.256 Å, which is longer by ~0.03 than the C=O in the uncoordinated 1,4-dihydroxyquinoxaline-2,3-dione [47]. Finally, the Mo–N bond lengths with an average value of 1.992 Å and compares well with those reported for M–N bond lengths of complexes containing *cis*-(bpy)₂M moiety [48,49].

The vibrational frequencies based on the optimized geometries were calculated and compared with the observed fundamental frequencies in Table 3. The optimized scale factors determined for $\text{Mo}_2(\text{bpy})_2(\text{DCQX})(\text{CO})_3$ complex was 0.998717. As can be seen in Table 3, the calculated harmonic vibrational frequencies compare well with the fundamental experimental frequencies. The calculated root mean square error (rms) per molecule is 34.19 cm^{-1} . The rms value compares very well with those reported for vibrational frequencies calculations using HF/6-311G(df,p), MP2-fc/6-311G(d,p) and B-LYP/6-31G(d) [50].

The ¹H NMR spectrum for the $\text{Mo}_2(\text{bpy})_2(\text{DCQX})(\text{CO})_3$ complex shown in Fig. 3 was very useful in assigning the coordination environments of the bipyridine ligands. The patterns shown in the spectrum is a typical of complexes containing *cis*-(bpy)₂M moiety [51–53]. Each bipyridine ligand in the complex has two magnetically inequivalent pyridine moieties and should result in two ABCD pyridine proton patterns for a total of eight chemical shifts. Only seven chemical shifts were observed and might be attributable to equivalence of the 3,3' protons in the bipyridine ligand [51,52]. The chemical shifts for the bipyridine protons (Fig. 3) were observed at 7.47 (t, 2H), 7.64 (t, 2H), 7.96 (t, 2H), 8.20 (t, 2H), 8.40 (d, 2H), 8.58–8.72 (m, 4H), 8.99 (d, 2H) ppm. On the other hand, the signal observed at 6.64 ppm (s, 2H) which was assigned to arene protons has shifted by 0.57 ppm to down field compared with the free ligand. Similar behavior was observed in the ¹H NMR spectra of benzene and $(\eta^6\text{-benzene})\text{Cr}(\text{CO})_3$ with chemical shifts at 7.36 and 5.26 ppm, respectively [54]. Evidently, the ¹H NMR results are in good support for the suggested structure **1** of the synthesized complex.

The data for thermal analysis (TGA), carried out on a solid sample of the $\text{Mo}_2(\text{bpy})_2(\text{DCQX})(\text{CO})_3$ complex in the temperature range 20–1000 °C at heating rate of 10 °C/min. under nitrogen atmosphere, are compiled in Table 4 and is characterized by five decomposition steps. The first step shows slow decomposition up to 164 °C with a net weight loss of 10.75% which is most probably due to loss of the three CO molecules. This is followed by gradual decomposition of one and half molecules of the bipyridine ligands in two steps in the temperature range 176–394 °C. The decomposition of the DCQX ligand was observed in the temperature range 408–572 °C. The last step covers the temperature range 782–991 °C with the elimination of the remaining of the bipyridine molecule. The remaining residue was found 23.17% which is best ascribed to two Mo metals.

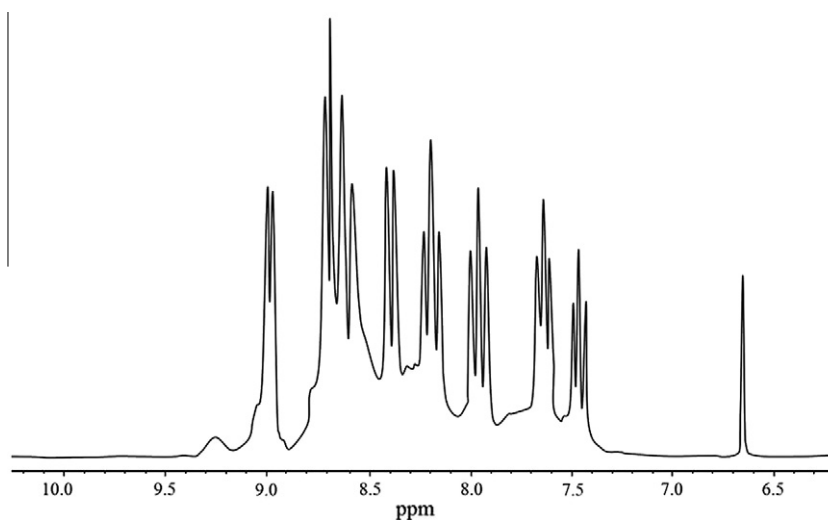


Fig. 3. The ¹H NMR spectrum for $\text{Mo}_2(\text{bpy})_2(\text{DCQX})(\text{CO})_3$ complex in $\text{DMSO-}d_6$.

Table 4
Thermal analysis data for Mo(bpy)₂(DCQX)(CO)₃ complex.

Decomposition steps (°C)	% Weight loss	Molecular weight (found)	Molecular weight (Calcd.)	Assigned species
78–164	10.75	88.07	88.06	3CO
176–305	19.02	155.80	156.18	1 bpy
310–394	9.47	77.53	78.09	1/2 bpy
408–752	28.44	232.96	233.05	DCQX + H ₂
782–991	9.16	75.00	76.08	1/2 bpy – H ₂

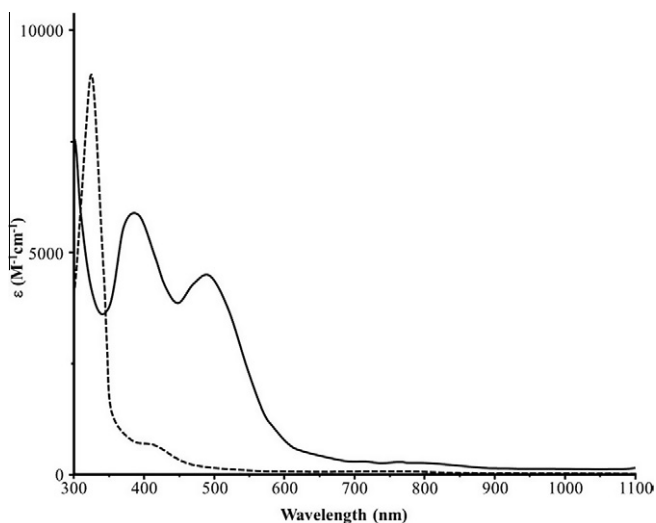


Fig. 4. The electronic absorption spectra measured in DMSO for DCQX ligand (.....) and Mo₂(bpy)₂(DCQX)(CO)₃ complex (—).

Table 5
Biological activities of DCQX ligand and Mo₂(bpy)₂(DCQX)(CO)₃ complex.

Sample	Inhibition zone diameter (mm/mg sample)			
	<i>Escherichia Coli</i> (gram-negative)	<i>Staphylococcus aureus</i> (gram-positive)	<i>Aspergillus flavus</i>	<i>Candida albicans</i>
DMSO ^a	0.0	0.0	0.0	0.0
Tetracycline ^b	31	33	–	–
Amphotericin B ^c	–	–	17	21
DCQX	15	16	12	12
Mo ₂ (bpy) ₂ (DCQX)(CO) ₃	18	18	14	15

^a DMSO solvent was used as negative control.

^b Standard antibacterial agent.

^c Standard antifungal agent.

The electronic absorption spectrum of the Mo₂(bpy)₂(DCQX)(CO)₃ is expected to be dominated by number of metal-to-ligand charge transfer transitions in addition to the intraligand (π – π^*) and ligand field (d – d) transitions. All the expected metal-to-ligand charge transfer transitions are of the type Mo(d_{π}) \rightarrow L(π^*), where L is CO, arene, and bipyridine ligands. It was reported that the electronic spectrum of Mo(bpy)(CO)₄ showed transitions due to Mo(d_{π}) \rightarrow bpy(π^*) and Mo(d_{π}) \rightarrow CO(π^*) at 462 and 257 nm, respectively [55]. And the arene molybdenum complex, (η^6 -C₇H₇)Mo(CO)₃, was reported to display Mo(d_{π}) \rightarrow arene(π^*) MLCT transition at 379 nm [56]. The electronic absorption spectrum of the free DCQX ligand and the Mo₂(bpy)₂(DCQX)(CO)₃ complex in DMSO solvent are shown in Fig. 4. The free ligand revealed two absorption at 324 and 410 nm attributable to the intraligand,

π – π^* and n – π^* transitions, respectively. The dominant feature of the electronic spectrum of the Mo₂(bpy)₂(DCQX)(CO)₃ complex is two broad absorption bands at 387 and 490 nm with molar absorption coefficient (ϵ , M^{–1}cm^{–1}) values of 5912 and 4491, respectively. These transitions, which are not present in the spectrum of the free ligand, can be assigned to the Mo(d_{π}) \rightarrow arene(π^*) and Mo(d_{π}) \rightarrow bpy(π^*) MLCT transition, respectively. The other Mo(d_{π}) \rightarrow CO(π^*) charge transfer transition, which is expected to occur in the higher energy region of the spectrum, was not observed due to the solvent cut off. Unfortunately, we were not able to study the solvatochromic effect on these charge transfer transitions due to the solubility problem of the complex in most common solvents. The ligand field transitions, expected at 393 and 344 nm, and are characteristic of Mo(0) complexes, might be obscured by the intense broad CT transitions [55,57]. In addition, the interligand (π – π^*) transition which is not observed in the spectrum of the complex has believed to be shifted to the higher energy region below 300 nm. This significant shift in the π – π^* transition to higher energy can be attributed to the localization of arene π -bonds which is a structural feature frequently observed upon coordination of an arene ligand to a metal center [45].

The antimicrobial activity of the DCQX ligand and its molybdenum complex were tested by the disc diffusion method against two types of pathogenic bacteria, namely, *S. aureus* and *E. Coli* by using DMSO as a solvent and tetracycline as a control. Also, the antifungal activity for the free ligand and the complex were tested against *A. flavus* and *C. albicans* fungi using Amphotericin as a control. The inhibition zone diameters for the antimicrobial activity were measured and the results are presented in Table 5. The results indicate that both DCQX ligand and Mo₂(bpy)₂(DCQX)(CO)₃ complex show biological activities against both bacteria and fungi. Although the inhibition zone diameters are lower than tetracycline and amphotericin B standards, the molybdenum complex showed higher inhibition activities against microorganisms compared with the free DCQX ligand. Interestingly, the molybdenum complex showed similar inhibition for Gram-positive and Gram-negative bacteria compared with the tetracycline that showed higher susceptibility for gram-positive bacteria which does not possess an outer cell membrane; therefore more susceptible.

References

- [1] C.W. Lindsley, Z. Zhao, W.H. Leister, R.G. Robinson, S.F. Barnett, D. Defeo-Jones, R.E. Jones, G.D. Hartman, J.R. Huff, H.E. Huber, M.E. Duggan, *Bioorg. Med. Chem. Lett.* 15 (2005) 761.
- [2] M. Loriga, S. Piras, P. Sanna, G. Paglietti, *Farmaco* 52 (1997) 157.
- [3] L.E. Seitz, W.J. Suling, R.C. Reynolds, *J. Med. Chem.* 45 (2002) 5604.
- [4] M.R. Myers, W. He, B. Hanney, N. Setzer, M. Maguire, A. Zulli, G. Bilder, H. Galzinski, A. Amin, S. Needle, A. Spada, *Bioorg. Med. Chem. Lett.* 13 (2003) 3091.
- [5] C. Bailly, S. Echepare, F. Gago, M. Waring, *Anti-Cancer Drug Des.* 14 (1999) 291.
- [6] S. Sato, O. Shiratori, K. Katagiri, *J. Antibiot.* 20 (1967) 270.
- [7] F.F. Becker, B.K. Banik, *Bioorg. Med. Chem. Lett.* 8 (1998) 2877.
- [8] F.P. Dwyer, E.C. Gyrfas, W.P. Rogers, J.H. Koch, *Nature* 170 (1952) 190.
- [9] F.P. Dwyer, E. Mayhew, E.M.F. Roe, A. Shulman, *Brit. J. Cancer* 19 (1965) 195.
- [10] F.P. Dwyer, I.K. Reid, A. Shulman, G.M. Laycock, S. Dixon, *Aust. J. Exp. Biol. Med. Sci.* 47 (1969) 203.
- [11] F.P. Dwyer, E.C. Gyrfas, R.D. Wright, A. Shulman, *Nature* 179 (1957) 425.
- [12] J.H. Koch, W.P. Rogers, F.P. Dwyer, E.C. Gyrfas, *Aust. J. Biol. Sci.* 10 (1957) 342.
- [13] H. Bregman, D.S. Williams, G.E. Atilla, P.J. Carroll, E. Meggers, *J. Am. Chem. Soc.* 126 (2004) 13594.
- [14] D.S. Williams, G.E. Atilla, H. Bregman, A. Arzoumanian, P.S. Klein, E. Meggers, *Angew Chem. Int. Ed. Engl.* 44 (2005) 1984–1987.
- [15] J.E. Debreczeni, A.N. Bullock, G.E. Atilla, D.S. Williams, H. Bregman, S. Knapp, E. Meggers, *Angew Chem., Int. Ed. Engl.* 45 (2006) 1580.
- [16] H. Thakuria, G. Das, *J. Chem. Sci.* 118 (2006) 425.
- [17] W.A. Bauer, W.M. Kirby, C. Sherris, M. Turck, *Am. J. Clin. Pathol.* 45 (1966) 493.
- [18] Hyperchem 6.01, Hypercube Inc. 2000.
- [19] E.C. Alyea, G. Ferguson, V.K. Jain, *Acta Cryst. C50* (1994) 491.
- [20] M.B. Hurthouse, M.A. Thornton-Pett, *Acta Cryst. C41* (1985) 184.
- [21] M. Wang, *Acta Cryst. E67* (2011) o1581.
- [22] S. Antonini, F. Calderazzo, U. Englert, E. Grigiotti, G. Pampaloni, P. Zanello, *J. Organomet. Chem.* 689 (2004) 2158.

- [23] G. Speier, Z. Tyeklar, P. Toth, E. Speier, S. Tisza, A. Rockenbauer, A.M. Walen, N. Alkire, C.G. Pierpont, *Inorg. Chem.* 40 (2001) 5653.
- [24] J.J.P. Stewart, *J. Mol. Model* 13 (2007) 1173.
- [25] A.P. Scott, L. Radom, *J. Phys. Chem.* 100 (1996) 16502.
- [26] M.H.B. Stiddard, *J. Chem. Soc.* (1962) 4712.
- [27] S.L. Vanatta, B.A. Duclos, D.B. Green, *Organometallics* 19 (2000) 2397.
- [28] S. Dilsky, P.K.B. Palomaki, J.A. Rubin, J.E. Saunders, R.D. Pike, M. Sabat, J.M. Keane, Y. Ha, *Inorg. Chim. Acta* 360 (2007) 2387.
- [29] M.H. Chisholm, J.A. Connor, J.C. Huffman, E.M. Kober, C. Overton, *Inorg. Chem.* 23 (1984) 2298.
- [30] K.J. Muir, G.P. McQuillan, W.T.A. Harrison, *Acta Cryst.* E63 (2007) m2491.
- [31] D. Astruc, *Organometallic Chemistry and Catalysis*, Springer-Verlag, Berlin Heidelberg, 2007.
- [32] K. Nakamoto, *Infrared and Raman Spectra of Inorganic and Coordination Compounds; Pt. B: Applications in Coordination, Organometallic, and Bioinorganic Chemistry*, Wiley-Interscience, sixth ed., USA, 2009.
- [33] F.A. Cotton, G. Wilkinson, C.A. Murillo, M. Bochmann, *Advanced Inorganic Chemistry*, sixth ed., John Wiley & Sons, New York, 1999.
- [34] R.S. Armstrong, M.J. Aroney, K.W. Nugent, *J. Mol. Struct.* 323 (1994) 15.
- [35] G. Davidson, E.M. Riley, *J. Organomet. Chem.* 19 (1969) 101.
- [36] D.M. Adams, A. Squire, *J. Chem. Soc. A* (1970) 814.
- [37] L.E. Orgel, *Inorg. Chem.* 1 (1962) 25.
- [38] R.E. Humphrey, *Spectrochim. Acta* 17 (1961) 93.
- [39] M. Ardon, G. Hogarth, D.T. Oscroft, *J. Organomet. Chem.* 689 (2004) 2429.
- [40] Y.J. Han, A.J. Lees, *Inorg. Chem. Acta* 147 (1988) 45.
- [41] A.S. Attia, *Spectrochim. Acta A* 67 (2007) 1339.
- [42] M.W. Lynch, M. Valentine, D.N. Hendrickson, *J. Am. Chem. Soc.* 104 (1982) 6982.
- [43] S. Antonini, F. Calderazzo, U. Englert, E. Grigiotti, G. Pampalonia, P. Zanello, *J. Organomet. Chem.* 689 (2004) 2158.
- [44] D.E. Koshland, S.E. Myers, J.P. Chesick, *Acta Cryst.* B33 (1977) 2013.
- [45] S.M. Hubig, S.V. Lindeman, J.K. Kochi, *Coord. Chem. Rev.* 200–202 (2000) 831.
- [46] C.G. Pierpont, R.M. Buchanan, *J. Am. Chem. Soc.* 97 (1975) 4912.
- [47] R. Abu-El-Halawah, B.F. Ali, M.M. Ibrahim, J.A. Zahra, W. Frey, *Acta Cryst.* E64 (2008) o571.
- [48] A. Baker, J. Jaud, J. Launay, J. Bonvoisin, *Inorg. Chim. Acta* 358 (2005) 3513.
- [49] L.E. Hansen, E.R. Glowacki, D.L. Arnold, G.J. Bernt, B. Chi, R.J. Fites, R.A. Freeburg, R.F.N. Rothschild, M.C. Krieg, W.A. Howard, J.M. Tanski, *Inorg. Chim. Acta* 348 (2003) 91.
- [50] K.K. Stavrev, M.C. Zerner, *J. Chem. Phys.* 102 (1995) 34.
- [51] B.P. Sullivan, D.J. Salmon, T.J. Meyer, *Inorg. Chem.* 17 (1978) 3334.
- [52] G.M. Bryant, J.E. Fergusson, *Aust. J. Chem.* 24 (1971) 441.
- [53] A.R. Rezvani, H. Hadadzadeh, B. Patrick, *Inorg. Chem. Acta* 333 (2002) 125.
- [54] A. Solladiecavallo, J. Suffert, *Org. Magn. Reson.* 14 (1980) 426.
- [55] A.B.P. Lever, *Inorganic Electronic Spectroscopy*, Second ed., Elsevier Science Publishers, B.V., 1984.
- [56] H. Hunkely, *Chem. Commun.* (1998) 397.
- [57] W. Kaim, W. Bruns, S. Kohlmann, M. Krejčík, *Inorg. Chim. Acta* 229 (1995) 143.